Article

Wildfire Risk Forecasting Using Weights of Evidence and Statistical Index Models

Ghafar Salavati [1], Ebrahim Saniei [1], Ebrahim Ghaderpour [2,*] and Quazi K. Hassan [2]

[1] Faculty of Rangeland and Watershed Management, Gorgan University of Agricultural Sciences and Natural Resources, Shahid Beheshti St Central Organization of the University, Gorgan 4913815739, Iran; ghafar_salavati@yahoo.com (G.S.); ebrahimsaniyi@gmail.com (E.S.)

[2] Department of Geomatics Engineering, Schulich School of Engineering, University of Calgary, 2500 University Drive NW, Calgary, AB T2N 1N4, Canada; qhassan@ucalgary.ca

* Correspondence: ebrahim.ghaderpour@ucalgary.ca

Abstract: The risk of forest and pasture fires is one of the research topics of interest around the world. Applying precise strategies to prevent potential effects and minimize the occurrence of such incidents requires modeling. This research was conducted in the city of Sanandaj, which is located in the west of the province of Kurdistan and the west of Iran. In this study, fire risk potential was assessed using weights of evidence (WoE) and statistical index (SI) models. Information about fire incidents in Sanandaj (2011–2020) was divided into two parts: educational data (2011–2017) and validation data (2018–2020). Factors considered for potential forest and rangeland fire risk in Sanandaj city included altitude, slope percentage, slope direction, distance from the road, distance from the river, land use/land cover (LULC), average annual rainfall, and average annual temperature. Finally, in order to validate the two models used, the receiver operating characteristic (ROC) curve was used. The results for the WoE and SI models showed that about 62.96% and 52.75% of the study area, respectively, were in the moderate risk to very high risk classes. In addition, the results of the ROC curve analysis showed that the WoE and SI models had area under the curve (AUC) values of 0.741 and 0.739, respectively. Although the input parameters for both models were the same, the WoE model showed a slightly higher AUC value compared to the SI model, and can potentially be used to predict future fire risk in the study area. The results of this study can help decision makers and managers take the necessary precautions to prevent forest and rangeland fires and/or to minimize fire damage.

Keywords: elevation; forecasting; geographic information system; Kurdistan; land use/land cover; statistical index; Sanandaj county; weights of evidence; wildfire risk; Zagros forests

1. Introduction

Wildfires are the result of interactions between several environmental factors, including fuel availability, weather, topography, and a source of ignition. When factors such as low humidity, strong wind, topography, and wind direction are favorable, a fire can rapidly develop if the quantity and availability of fuel are appropriate [1]. Forest fire risk is a term used to describe the possibility of vegetation (i.e., land cover) causing the ignition and spread of a fire through fuel characteristics, such as the type, load, and moisture content [2]. In other words, the risk of wildfire also depends on the characteristics of vegetation, such as forests with many oil trees, vines, or branches with dry leaves [3]. The terms risk, danger, and hazard have been used in the literature since the beginning of modern fire science in the 1920s [4,5].

Wildfire risk is considered one of the main reasons for the decline of forest ecosystems around the world, which can occur naturally or as a result of human intervention [6]. Wildfire is a critical Earth-system process that has significant influences on both terrestrial and atmospheric conditions, especially in relation to vegetation dynamics, biogeochemical

cycling, and atmospheric chemistry [7]. As a common and prevalent disturbance that affects the environment, economy, and social life, forest fires not only damage the trees, but also the whole forest ecosystem by altering the vegetation composition, structure, and biogeochemical cycle [8]. Proper planning is needed to reduce fire risk, restore the fire regime, and manage forest fires effectively.

Despite the impacts of wildfire in terms of degradation, such as the reduction of plant communities and biodiversity, which can accelerate deforestation processes [9], wildfires also play essential roles in many forest processes. For example, forest fires influence the composition and successional stages [10], and they act as a selective factor for the traits of plants [11]. Forest fires have an impact on many other Earth-system processes, such as the carbon and nutrient cycles, the atmospheric cycle regulating the oxygen content of the atmosphere, and the evolutionary processes of many plant species [12]. Other advantages of forest fires are the elimination of harmful microorganisms, fungi, insects, and herbal diseases, as well as soil enrichment with the nutrients and minerals released from the remaining ash [13].

According to the literature, the spatial factors affecting wildfires are climatic factors, such as wind speed, wind direction, rainfall, humidity, temperature, solar radiation, and seasonal changes [14,15], morphological factors, such as slope, aspect, curvature, indicators of topography, altitude, distance from the river, distance from human-made facilities, and soil moisture and texture [16], and parameters related to the type of fuel, including the condition and type of tree, type of land cover, and cover density [17–20].

In 2015, approximately 98 million hectares of forest around the world were affected by fires [21]. Based on the results of some studies, the occurrence of future climate change and its effects on rainfall patterns and the occurrence of drought will intensify forest fires in many places [20,22,23], which, in turn, increases the demand for managers to adopt fire risk reduction strategies in the face of future climate change. Numerous factors increase the incidence of forest fires around the world, such as tourist imprudence by lighting campfires in forests, deliberate fires used to convert forest lands into agricultural lands [24,25], traditional agricultural practices, such as residual burning, lightning-induced fires [20,26], droughts, hot winds [27,28], smoking [29], and the release of bottles or broken glass, which work as a collective lens that focuses the sun light [30].

The Zagros forests are located in the west and southwest of Iran and along the Zagros mountains. The area of these forests is about six million hectares, covering about 44% of Iran's forests. In the Zagros forests, there are about 170 species of trees and shrubs. *Quercus libani, Quercus infectoria, Pistacia atlantica, Amygdalus, Crataegus,* and *Celtis australis* are important wood species in the Zagros region [31].

According to a report published by the Natural Resources and Watershed Management Organization of Iran, forest and rangeland fires occur frequently, and fires in the forests of Iran have destroyed a large part of these valuable ecosystems in recent years. Iran is one of the lowest-forest-cover countries in the world. Therefore, the investigation of the consequences of forest fires in the forests of Iran and the recognition of fire suppression methods for fires in these forests are essential in order to present a solution for decreasing these fires [32]. Reports indicate the occurrence of 1124 cases of fires and the burning of 7364 hectares of forests and rangelands of the Kurdistan province between only 2007 and 2016 [33].

Herein, the study area is a part of the Zagros forests of western Iran, which are dominated by oak trees. In recent years, the area of the Zagros forests has decreased, which is mainly due to climate change. The effect of climate change on reducing the area of the Zagros forests has been confirmed in various studies [34,35]. Furthermore, climate change and the rise of the mean annual temperature have increased the fire rate in forests and pastures. It seems that the fire affects the vegetation and changes the forest stand structures. The results of the study in [36] showed that, a decade after the occurrence of a fire, the share of oak trees was decreased, while the proportions of *Amygdalus* and *Crataegus* were increased.

As reported by forest managers, forest fire models depend on the stages of the fire: pre-fire planning (fire risk modeling), fire control (fire behavior modeling), and post-fire assessment (effects of fire and economic models) [26,37]. Sensitivity zoning is a vital component of forest fire management. The methods used to assess potential fire risk can be divided into four categories: (i) statistical and data-driven models, (ii) machine learning models, (iii) multi-criteria decision models, and (iv) hybrid models. The results show that data-driven models are the most common methods for assessing the potential of forest fire risk, but hybrid models are the most accurate methods [38].

Common methods used to potentially model the risk of forest and rangeland fires include hierarchical analysis [39,40], particle swarm optimization [41], the statistical index (SI) [40], differential evolution algorithm [41], functional data analysis (FDA) [42], generalized linear model (GLM) [43], support vector machine (SVM) and artificial neural network (ANN) [43], random forest [43,44], frequency ratio [45,46], fuzzy analytic network process [47], VIKOR and Topsis [48], definitive evidence function [2], weights of evidence (WoE) [46,49], logistic regression [41,50], spectral and wavelet analyses [15,51], dynamic four-day scale forecast modeling [5], and complex mathematical models, such as elmfire [52]. Each method has its own advantages and weaknesses.

Fires in the Zagros forests have been studied by many researchers. In research conducted in the Sardasht forests, it was shown that wildfires have a higher chance of occurring between June and September [53]. In another study, fire danger maps were created using an SVM, GLM, FDA, and random forest. The results of that study showed that the FDA (0.777) and GLM (0.772) algorithms generated the most accurate fire danger maps [54]. Jaafari et al. [55] modeled wildfire probability across the Zagros mountains of Iran using the WoE model. The findings of that study clearly demonstrated that the probability of a fire was strongly dependent on the topographic characteristics of landscapes and, perhaps more importantly, human infrastructure and associated human activities.

The main advantage of the WoE and SI models is that they calculate the weighted values of the factors based on a statistical formula, so they avoid the subjective choice of weighting factors. In addition, input maps with missing data (incomplete coverage) can be accommodated in the models, which does not significantly impact the results [40,56]. However, the main shortcoming of the WoE and SI models is that the weight values calculated for different areas are not comparable in terms of the degree of hazard [56].

In Iran, wildfires are seen as a significant threat to forests and pastures. Some estimates suggest that an average of 400 fire events occur per year, burning over 6000 hectares of land [57]. This trend is expected to continue and may even increase in the future due to ongoing climate and land-use changes, as well as increasing human activities [58]. On the other hand, and based on many surveys that have been conducted, the application of the WoE and SI models in forest fire susceptibility mapping is novel. Therefore, this research was conducted to evaluate the WoE and SI models for wildfire susceptibility mapping in Sanandaj county. In other words, the aim of this study was to identify high-risk and low-risk areas of wildfires in the study area using the WoE and SI models in order to manage and reduce the risk of fire. Maps of factors affecting fires, including altitude, slope percentage, slope direction, distance from the road, distance from the river, land use/land cover (LULC), average annual rainfall, and average annual temperature, were prepared using the available statistical data (2011–2020) and a geographic information system (GIS). Then, with the help of mathematical functions (WoE and SI models), a fire potential map for the area was forecasted, and finally, the two models were compared using their ROC curves.

The rest of the paper is organized as follows. In Section 2, the study region, datasets, preprocessing, methods, and evaluation criteria are described. The results are demonstrated in Section 3. The results are discussed and compared with those of other similar studies in Section 4. Finally, Section 5 concludes this paper.

2. Materials and Methods

2.1. Study Region

This research was conducted in Sanandaj city, which is located in the west of Kurdistan province and the west of Iran. With an area of 231,721 hectares, Sanandaj city is located between $47°14'41''$ and $46°24'55''$ east longitude and $35°38'25''$ to $35°2'26''$ north latitude. The location of the study area in Kurdistan and Iran is shown in Figure 1. The areas of the forests and rangelands of Iran are 17,649,890 and 83,309,167 hectares (ha), respectively; among these, the areas of forests and rangelands of Kurdistan province are 256,794 and 1,182,214 ha, respectively [59]. The study region has a Mediterranean climate, and with the onset of summer, many scattered fires occur in pastures and forests. In recent years, climate change has had a negative impact, and the number and extent of fires have increased. Therefore, the development of accurate strategies for preventing potential effects and minimizing the occurrence of such incidents requires modeling.
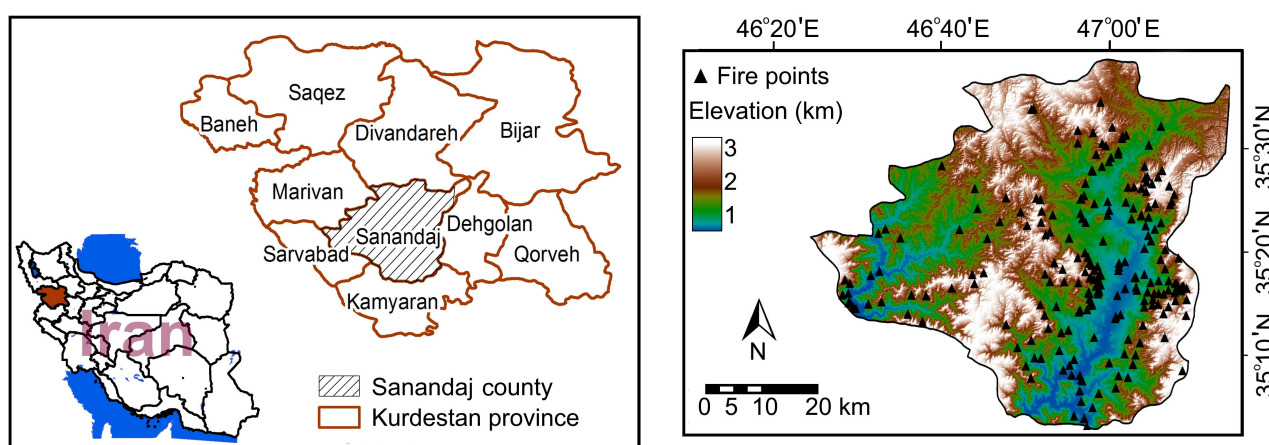

Figure 1. Map of the study region showing the location of Sanandaj in Kurdistan and Iran.

2.2. Dataset and Preprocessing

Data related to fire incidents in Sanandaj city (2011–2020) were provided by the Natural Resources and Watershed Management Department of Sanandaj city. In the first step, the fire incidents were divided into two parts: educational data (2011–2017) and validation data (2018–2020). In order to prepare a fire risk zoning map, the factors affecting the occurrence of fires in the area were first identified. Factors considered for potential forest and rangeland fire risk in Sanandaj city included altitude, slope percentage, slope direction, distance from the road, distance from the river, LULC, average annual rainfall, and average annual temperature [14,16].

Topographic variables, such as altitude, slope, and aspect, affect the behavior and speed of forest fires' spread [60]. These topographic variables were derived from a digital elevation model (DEM) with a resolution of 12.5×12.5 square meters, which was downloaded from the advanced land-observing satellite (ALOS PALSAR) and from the Alaska satellite facility [61].

2.3. Methods

2.3.1. Maps and Layers

One of the effective factors in the occurrence of forest and pasture fires is altitude; with increasing altitude, fire risk decreases [62]. The height class maps were obtained by using the digital model of the height with a pixel size of 12.5×12.5 square meters. There is a direct relationship between the land slope factor and fire risk potential; with increasing land slope, fire risk increases [62]. These maps were prepared based on the DEM and were classified into six classes. An aspect map is an important factor in wildfire occurrence. South-facing aspects receive more sunlight, higher temperatures, robust winds, low humidity, and low

fuel moisture in the Northern Hemisphere [27], which could potentially be in favor of fire occurrences. These maps were also prepared based on the DEM and were classified into nine classes.

The LULC layer was prepared by the Forests and Rangelands Organization. The LULC layer was also divided into different classes based on the different uses. Climatic variables are among the main factors affecting the occurrence of forest fires because they affect the quality and quantity of flammable materials [13,26]. There is a direct relationship between temperature and fire risk; the higher the temperature, the higher the fire risk [63]. Meteorological data on temperature and precipitation were provided by the Meteorological Organization. To prepare isothermal and precipitation maps, 20-year meteorological data (2001–2020) from the synoptic meteorological and climatological stations of Kurdistan province were used, and the desired maps were prepared using the inverse-distance-weighted (IDW) interpolation method. Maps of distances from rivers and roads were prepared using a 1:50,000 digital topographic map and through the application of distance functions (Figure 2).

2.3.2. Weights of Evidence (WoE)

The evidence weighting or conditional probability method was first developed to identify and explore mineral deposits [64]. The evidence weighting method is a data-driven method used to combine datasets, and it is based on the use of a linear form of the Bayesian probability model for the estimation of the relative importance of evidence using statistics [65]. Let N_{pix1} be the number of pixels with fire in the class, let N_{pix2} be the number of pixels with fire in the map minus the number of pixels with fire in the class, let N_{pix3} be the number of pixels in the class minus the number of pixels with fire in the class, and let N_{pix4} be the total number of pixels in the map minus the number of pixels with fire in the map minus the number of pixels in the class plus the number of pixels with fire in the class. The weights in the WoE are determined with Equations (1) and (2) [66,67].

$$W_i^+ = \ln\left(\frac{N_{\text{pix1}}}{N_{\text{pix1}} + N_{\text{pix2}}} \middle/ \frac{N_{\text{pix3}}}{N_{\text{pix3}} + N_{\text{pix4}}}\right) \tag{1}$$

$$W_i^- = \ln\left(\frac{N_{\text{pix2}}}{N_{\text{pix1}} + N_{\text{pix2}}} \middle/ \frac{N_{\text{pix4}}}{N_{\text{pix3}} + N_{\text{pix4}}}\right) \tag{2}$$

A positive weight W^+ indicates that there is a causal agent at the site of the fire, and the magnitude of this weight indicates the correlation between that agent and the occurrence of the fire. However, a negative weight W^- indicates the absence of the desired factor at the site of the fire, indicating a negative level of correlation. The difference between positive and negative weights indicates the magnitude of the spatial relationship between the causative agent and the occurrence of a fire, as calculated with Equation (3) [68].

$$WF = W^+ - W^-. \tag{3}$$

To obtain the final weight of each factor, the positive and negative weights of the various classes of each factor are added together. If the weight of the factor is positive, it plays a role in the occurrence of a fire, and if the weight of the factor is negative, it indicates that the factor has no effect on the occurrence of a fire. Some factors also have a small effect on the occurrence of fires, and their weight is zero or close to zero. From the weights, a weighted thematic map was obtained, and a fire prediction map was calculated.

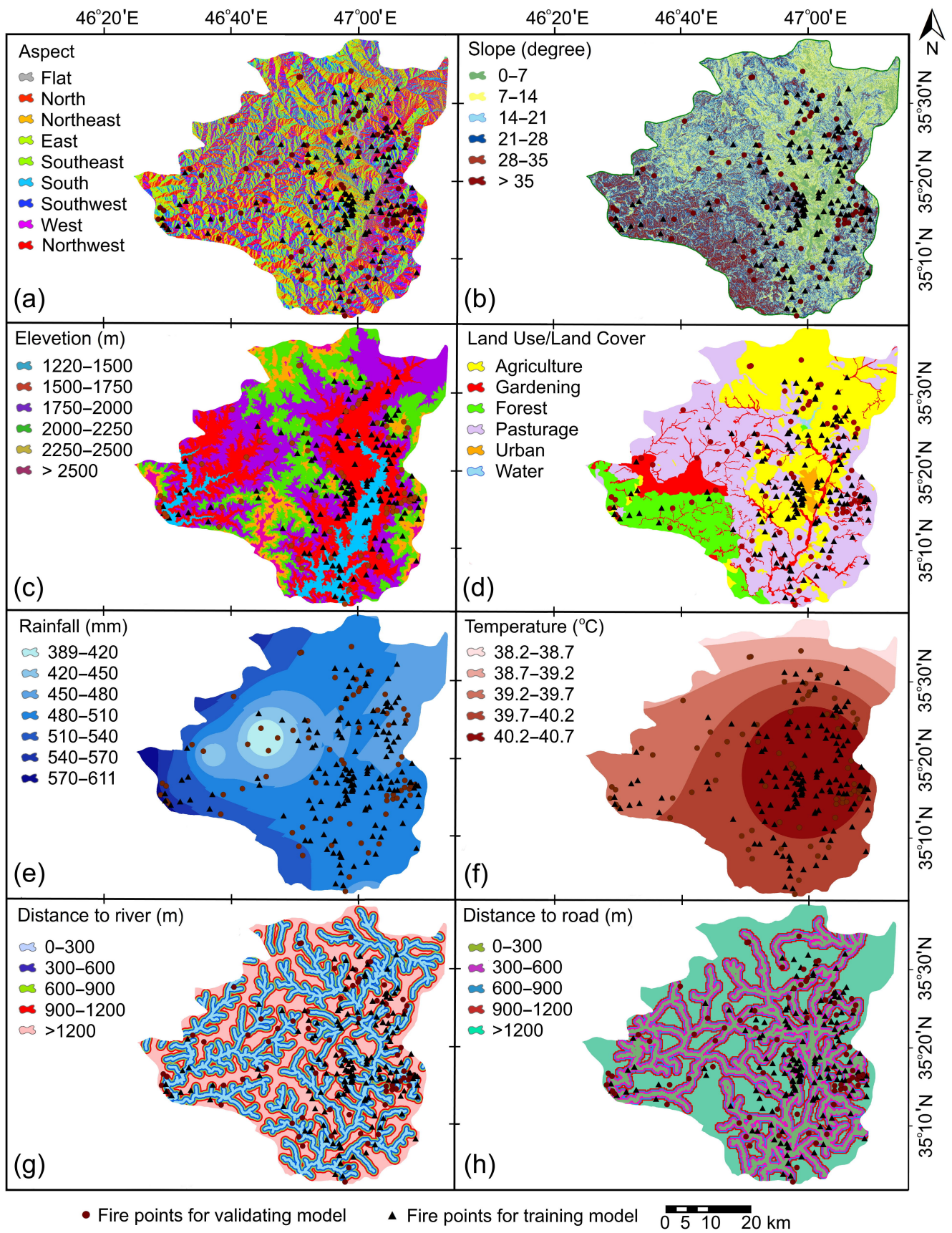**Figure 2.** Wildfire ignition factors used in this study: (**a**) aspect, (**b**) slope, (**c**) elevation (m), (**d**) LULC, (**e**) rainfall (mm), (**f**) temperature (°C), (**g**) distance to rivers (m), and (**h**) distance to roads (m) maps.

2.3.3. Statistical Index (SI)

The statistical index method is a two-variable statistical method that was first proposed by van Westen [69] for landslide sensitivity maps. Definite weight values for each of the classes of parameters affecting the occurrence of fires are obtained as the natural logarithm of the fire density in each class divided by the fire density in the whole map. The statistical index method is a bi-variate statistical method. Certain weight values for each of the classes of effective parameters in the fire risk zoning are obtained as the natural logarithm of the fire density in each class divided by the fire density in the whole map. The formula of the SI model is given by

$$W_{\mathrm{SI}} = \ln \left(\frac{F_{ij}}{P_{ij}} \Big/ \frac{F_{\mathrm{T}}}{P_{\mathrm{T}}} \right), \tag{4}$$

where W_{SI} is the weight given to a certain class i of factor j; F_{ij} is the number of forest fires in a certain class i of factor j; F_{T} is the total number of forest fires in the study area; P_{ij} is the number of pixels in a certain class i of factor j; P_{T} is the total number of pixels in the study area [40]. The values obtained for each class were used in GIS in the relevant layers, and a fire risk zoning map was obtained. Finally, the prepared map was divided into five hazard classes, namely, very low, low, moderate, high, and very high risk.

2.4. Evaluation Criteria

In this study, using the receiver operating characteristic (ROC) curve, the performance of each model was investigated. The ROC curve is the most widely used statistical technique for assessing the efficiency of models [70]. The ROC curve is a graph technique for examining the trade-off between specificity and sensitivity, with the x-axis showing a false-positive rate (1-specificity) and the y-axis showing a true-positive rate (sensitivity). The area under the ROC curve is called the area under the curve (AUC), and the model with the highest AUC has the highest relative performance. An AUC of 0.5 is equivalent to a neutral model, and the closer this value is to one, the higher the model efficiency [71]. The interpretation of ROC values includes negligible, poor, moderate, good, very good, and excellent with ROC values of $0 < \mathrm{AUC} \le 0.5$, $0.5 < \mathrm{AUC} \le 0.6$, $0.6 < \mathrm{AUC} \le 0.7$, $0.7 < \mathrm{AUC} \le 0.8$, $0.8 < \mathrm{AUC} \le 0.9$, and $0.9 < \mathrm{AUC}$, respectively [72,73].

3. Results

The results of the relationship between each of the effective factors and the occurrence of fires using the WoE and SI models are presented in Table 1. As can be seen, the southeast (1.43) and flat (0.0) directions had the highest impact and the lowest impact on fire occurrence, respectively. In addition, slopes of 0–7 degrees (1.35) and 14–21 degrees (0.76) had the highest and lowest impacts on the occurrence of fires, respectively. On the other hand, the highest number of fires was observed at the altitude floor of 1218–1500 m (2.07), and the lowest number of fires was observed at the altitude floor of more than 2500 m (0.00). As the distance from the river increased, the probability of fires increased, and the highest number of fires was observed at a distance of more than 1200 m (1.12). In addition, according to the results of weighting, there was an inverse relationship between the distance from the road and the potential for fire, i.e., the shorter the distance from the road, the higher the probability of a potential fire. Examination of the LULC map showed that fires occurred more in lands with urban use (2.41), and then agricultural use (1.26). The highest incidence of fires was observed in rainfall classes of 480–510 mm (1.37), and the lowest incidence of fires was observed in classes with the lowest rainfall. The highest positive correlation was observed between the occurrence of fires and the temperature parameter at temperatures higher than 40.2 °C (1.99).

The fire potential maps obtained by using the WoE and SI models are illustrated in Figure 3. The areas and percentages of floor areas for potential fire occurrence are listed in

Table 2. The results of the WoE and SI models showed that about 62.96% and 52.75% of the study area were in the moderate, high, and very high fire potential classes, respectively.

Table 1. Percentages of numbers of pixels and fire points, as well as the score classes of parameters in the WoE and SI models.

| Factor	Class	Pixels (%)	Fire (%)	W^+	W^-	WF	W_{SI}
Aspect	Flat	0.00	0.00	0.00	0.00	0.00	0.00
	North	0.11	0.12	0.06	−0.01	0.07	1.06
	Northeast	0.12	0.12	−0.04	0.01	−0.04	0.96
	East	0.13	0.14	0.12	−0.02	0.14	1.13
	Southeast	0.13	0.19	0.36	−0.07	0.43	1.43
	South	0.13	0.10	−0.28	0.04	−0.31	0.76
	Southwest	0.14	0.13	−0.10	0.02	−0.12	0.90
	West	0.13	0.09	−0.30	0.04	−0.34	0.74
	Northwest	0.11	0.12	0.05	−0.01	0.06	1.05
Slope (degree)	0–7	0.13	0.18	0.34	−0.06	0.41	1.35
	7–14	0.24	0.22	−0.09	0.03	−0.12	0.87
	14–21	0.28	0.23	−0.23	0.08	−0.30	0.76
	21–28	0.23	0.24	0.04	−0.01	0.05	0.99
	28–35	0.12	0.13	0.12	−0.02	0.14	1.08
	>35	0.04	0.05	0.04	0.00	0.04	0.99
Elevation (m)	1218–1500	0.08	0.17	0.73	−0.10	0.83	2.07
	1500–1750	0.27	0.38	0.32	−0.15	0.47	1.37
	1750–2000	0.33	0.23	−0.34	0.13	−0.47	0.71
	2000–2250	0.22	0.19	−0.12	0.03	−0.16	0.88
	2250–2500	0.08	0.03	−1.08	0.06	−1.13	0.34
	>2500	0.02	0.00	0.00	0.02	−0.02	0.00
Distance to river (m)	0–300	0.38	0.22	−0.53	0.22	−0.75	1.02
	300–600	0.27	0.15	−0.57	0.15	−0.73	0.80
	600–900	0.17	0.19	0.11	−0.02	0.13	1.10
	900–1200	0.11	0.13	0.16	−0.02	0.18	0.90
	>1200	0.07	0.30	1.50	−0.29	1.79	1.12
Distance to road (m)	0–300	0.24	0.39	0.50	−0.23	0.73	1.65
	300–600	0.16	0.22	0.31	−0.07	0.38	1.36
	600–900	0.10	0.09	−0.02	0.00	−0.02	0.98
	900–1200	0.11	0.08	−0.39	0.04	−0.43	0.68
	1200–10,600	0.39	0.22	−0.60	0.25	−0.85	0.55
LULC	Agriculture	0.31	0.40	0.24	−0.13	0.37	1.26
	Gardening	0.10	0.09	−0.14	0.01	−0.16	0.87
	Forest	0.12	0.04	−0.97	0.08	−1.05	0.38
	Pasturage	0.45	0.44	−0.03	0.02	−0.05	0.97
	Urban	0.01	0.03	0.88	−0.02	0.90	2.41
	Water	0.00	0.00	0.00	0.00	0.00	0.00
Rainfall (mm)	389–420	0.02	0.00	0.00	0.02	−0.02	0.00
	420–450	0.05	0.02	−1.01	0.03	−1.04	0.36
	450–480	0.24	0.22	−0.11	0.03	−0.14	0.90
	480–510	0.52	0.71	0.31	−0.51	0.82	1.37
	510–540	0.14	0.03	−1.43	0.12	−1.54	0.24
	540–570	0.03	0.02	−0.41	0.01	−0.42	0.66
	570–611	0.01	0.01	−0.49	0.00	−0.50	0.61
Temperature (°C)	38.18–38.7	0.03	0.00	0.00	0.03	−0.03	0.00
	38.7–39.2	0.09	0.00	0.00	0.10	−0.1	0.00
	39.2–39.7	0.26	0.23	−0.13	0.04	−0.17	0.66
	39.7–40.2	0.36	0.10	−1.29	0.35	−1.64	0.21
	40.2–40.7	0.25	0.67	0.98	−0.81	1.79	1.99
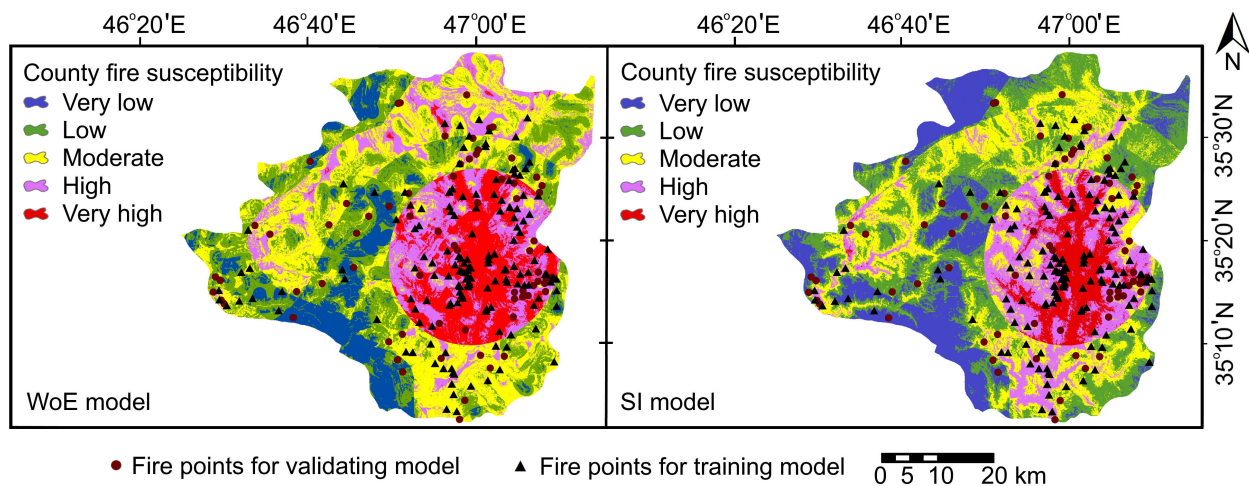
Figure 3. Maps of the fire hazard potential using the WoE model (**left** panel) and SI model (**right** panel).

Table 2. Area and percentage of area of fire potential classes based on the WoE and SI models.

Classes	WoE Area (ha)	WoE Area (%)	SI Area (ha)	SI Area (%)
Very low	34,751	11.79	51,340	17.42
Low	74,398	25.25	87,895	29.83
Moderate	88,162	29.92	76,487	25.96
High	56,852	19.29	54,119	18.37
Very high	40,504	13.75	24,825	8.42

The ROC curve was used to validate the fire potential maps. The AUC values for the models that were evaluated according to the validation data are presented in Table 3. In addition, the ROC curve of the models that were evaluated according to the validation data is illustrated in Figure 4. Of the WoE and SI models under study, the highest accuracy was attributed to the WoE model (0.741); therefore, in terms of fire potential detection, the WoE model had a slightly better performance than the SI model.
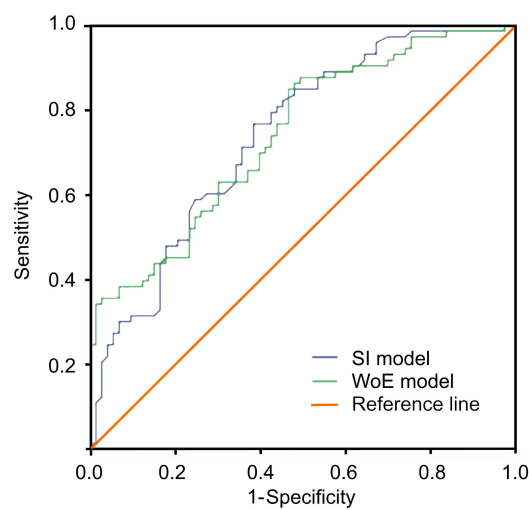

Figure 4. The ROC curves of the WoE and SI models with respect to the validation data.

Table 3. AUC values of the models for predicting fire potential.

Validation Data	Prediction Model
WoE	0.741
SI	0.739

4. Discussion

As one of the most important causes of natural disturbances in forest ecosystems, fire has a great impact on forest resources, climate change, and ecological sequences [74]. Knowledge of fire-prone areas with fire potential is essential for regional and logistical planning, as well as fire prevention and control measures [75]. Herein, the relationship between each of the effective factors and the points of occurrence of fires was investigated using the WoE and SI models.

Kayet et al. [76] stated that the highest correlation between fire occurrence and slope measurement criteria was observed in the southwest and southeast directions. This finding is consistent with the results of the current study. As was observed, the southeast direction (1.43) had the greatest impact on the occurrence of fires, which was consistent with the findings of the study by Hong et al. [77]. The slope plays an important role in fires, and the speed of a fire tends to increase on steep slopes. The slopes of 0–7 and 28–35 degrees had the greatest impact on the occurrence of fires, but in the study of Hong et al. [77], a slope of more than 30 degrees had the greatest impact on the occurrence of fires.

Elevation above sea level affects the extent of a fire by changing the shape of the front and the process of the spreading of the fire. In a study in Greece, the height and density of vegetation were found to affect the spread of fires [78]. The highest number of fires was observed on the lowest elevation floor (1218–1500 m), and the number of fires decreased with increasing altitude. In the study conducted by Hong et al. [77], the highest score obtained from the WoE model was observed in the highest elevation class, which contradicts the results of the current study. In addition, in another study, the highest score obtained from the weights of evidence model was observed in the middle altitude class (400–600 m) [46]. In other studies, the highest correlation between fire incidence and altitude was observed at the lowest elevation [16,76], which was consistent with the results of the current study.

The vegetation water content is closely related to the forest fire situation, such that with drought occurrence and the drying of seasonal rivers or an increase in distance from water sources, such as rivers, vegetation loses its moisture, which leads to conditions that can potentially increase the chance of fire occurrence [20,79]. According to the results of the current study, with increasing distance from a river, the probability of fire increased, which is consistent with the results of the study by Hong et al. [46].

Sensitivity to forest fires is directly related to proximity to roads and footpaths. Road corridors significantly affect the spatial patterns of human-induced fires [80]. There is an inverse relationship between the distance from a road and the potential for fire, i.e., the longer the distance from the road, the lower the probability of fire. The results of the study by Hong et al. [46,77] showed that the highest probability of fires occurred on the floor at the altitude of 500–1500 m. Vegetation characteristics and LULC types are major and effective factors in fires [16,20,81]. Examination of the LULC map showed that fires occurred more in urban lands (2.41), and then agricultural lands (1.26). The reason for this is probably the occurrence of fires in forest parks within the city of Sanandaj. The results of the study by Hong et al. [77] showed that the highest correlation was between fire occurrence and forest and residential uses.

The highest score of the models was observed in the middle rainfall classes (480–510 mm), and the lowest score was observed in the classes with the lowest rainfall. Hong et al. [46] achieved similar results and stated that the highest correlation between fire occurrence and rainfall classes was observed in the middle rainfall classes (1200–1300 mm). A direct relationship was observed between the occurrence of fires and the temperature parameter, such

that with increasing temperature, the correlation between fire occurrence and temperature increased. This finding is consistent with the results of the studies by Ahmed et al. [14] and Hong et al. [46].

In this study, the WoE and SI models were used to assess potential forest and rangeland fire risk. In a study conducted in Turkey, the potential for fire risk was investigated using an SI model and a hierarchical analysis approach. The results of this study showed that the SI model had good performance for potential fire risk [40]. The results of the proposed models showed that the highest accuracy belonged to the WoE model (0.741); therefore, in terms of fire potential detection, the WoE model performed slightly better than the SI model. Sivrikaya et al. [40] examined the performance of hierarchical analysis and SI models for potential fire risk in Turkey. The results of their study showed that the SI model had good performance for potential fire risk. Juliev et al. [82] stated that the SI model had a good performance for potential landslide risk matching, which is consistent with the results of the present study.

The results of the WoE and SI models in this study showed that about 62.96% and 52.75% of the study area were in the medium to very high risk classes, respectively. Eugenio et al. [83] used SI models to map forest fire risk. Their results for Espírito Santo State in Brazil showed approximately 3.81% low risk, 21.18% medium risk, 30.10% high risk, 41.50% very high risk, and 3.40% severe forest fire risk, and in total, high, very high, and extreme risk areas accounted for 78.92% of heat spots. Hong et al. [77] examined the spatial patterns of fire sensitivity in China. The results of their study showed that the WoE model had good performance (0.854) for potential fire risk. In another study conducted in China, Hong et al. [46] examined the potential for fire risk using frequency ratio, WoE, and linear and quadratic differential analysis models. The WoE model had the highest yield (2.82). Other researchers have endorsed the performance of the WoE model for the spatial modeling of hazards.

According to the information related to fires that occurred in Sanandaj city, the occurrence of fires in forest parks inside Sanandaj city, as well as in the rangelands and forest lands on the outskirts of Sanandaj city, was significant. On the other hand, one of the effective factors in the occurrence of forest fires is population density or proximity to population centers. Previous studies showed that most forest fires occurred near densely populated areas of Spain and Portugal [84,85].

5. Conclusions

In this study, WoE and SI models were used to assess potential fire risk in Sanandaj, Iran. To prepare a fire sensitivity map, information related to the fires that occurred and the effective factors of these events, including altitude, slope, aspect, LULC, distance from a river, distance from a road, annual rainfall, and maximum annual temperature, were used. The results showed that the WoE model (0.741) had slightly better performance than that of the SI model (0.739) for fire risk. In general, it can be concluded that these two models have good performance for potential fire risk.

According to the wildfire risk forecasting map, the highest number and density of forest fires occurred in the lands and forest parks around Sanandaj city, where the human factor had the greatest role in these fires. Therefore, in order to prevent and deal with potential hazards due to fires in areas containing natural resources and environments in Sanandaj city, measures should be taken to increase monitoring in areas with high and very high fire risk potential, such as by increasing the amount of human resources, creating firebreaks, and allocating most of the financial resources related to forest and rangeland firefighting, i.e., by launching an appropriate fire extinguishing system, using modern technologies and appropriate equipment, and training expert forces. Other strategies for preventing fires in fields of natural resources and the environment include building a culture around the importance and use of these national resources. The fire risk potential maps prepared in this study may be used as a very effective management tool for developing fire risk reduction strategies and management measures in order to reduce fire events in areas with high and very high risk of fires.

Abbreviations

The following abbreviations are used in this manuscript:

ANN	Artificial Neural Network
AUC	Area Under the Curve
DEM	Digital Elevation Model
FDA	Functional Data Analysis
GIS	Geographic Information System
GLM	Generalized Linear Model
IDW	Inverse Distance Weighted
LULC	Land Use/Land Cover
ROC	Receiver Operating Characteristic
SI	Statistical Index
SVM	Support Vector Machine
WoE	Weights of Evidence

References

1. Wen, C.; He, B.; Quan, X.; Liu, X.; Liu, X. (Eds.) Wildfire Risk Assessment Using Multi-Source Remote Sense Derived Variables. In Proceedings of the IGARSS 2018–2018 IEEE International Geoscience and Remote Sensing Symposium, Valencia, Spain, 22–27 July 2018; IEEE: Piscataway, NJ, USA, 2018.
2. Nami, M.; Jaafari, A.; Fallah, M.; Nabiuni, S. Spatial prediction of wildfire probability in the Hyrcanian ecoregion using evidential belief function model and GIS. *Int. J. Environ. Sci. Technol.* **2018**, *15*, 373–384. [CrossRef]
3. Keane, R.E.; Drury, S.A.; Karau, E.C.; Hessburg, P.F.; Reynolds, K.M. A method for mapping fire hazard and risk across multiple scales and its application in fire management. *Ecol. Model.* **2010**, *221*, 2–18. [CrossRef]
4. Çolak, E.; Sunar, F. Evaluation of forest fire risk in the Mediterranean Turkish forests: A case study of Menderes region, Izmir. *Int. J. Disaster Risk Reduct.* **2020**, *45*, 101479. [CrossRef]
5. Ahmed, M.R.; Hassan, Q.K.; Abdollahi, M.; Gupta, A. Introducing a new remote sensing-based model for forecasting forest fire danger conditions at a four-day scale. *Remote Sens.* **2019**, *11*, 2101. [CrossRef]
6. Sachdeva, S.; Bhatia, T.; Verma, A., GIS-based evolutionary optimized Gradient Boosted Decision Trees for forest fire susceptibility mapping. *Nat. Hazards* **2018**, *92*, 1399–1418. [CrossRef]
7. Merino-de-Miguel, S.; González-Alonso, F.; Huesca, M.; Armenteras, D.; Franco, C. MODIS reflectance and active fire data for burn mapping in Colombia. *Earth Interact.* **2011**, *15*, 1–17. [CrossRef]
8. Chaparro, D.; Vall-Llossera, M.; Piles, M.; Camps, A.; Rüdiger, C.; Riera-Tatché, R. Predicting the extent of wildfires using remotely sensed soil moisture and temperature trends. *IEEE J. Sel. Top. Appl. Earth Obs. Remote Sens.* **2016**, *9*, 2818–2829. [CrossRef]
9. Ahn, Y.S.; Ryu, S.R.; Lim, J.; Lee, C.H.; Shin, J.H.; Choi, W.I.; Lee, B.; Jeong, J.-H.; An, K.W.; Seo, J.I. Effects of forest fires on forest ecosystems in eastern coastal areas of Korea and an overview of restoration projects. *Landsc. Ecol. Eng.* **2014**, *10*, 229–237. [CrossRef]
10. Huebner, K.; Lindo, Z.; Lechowicz, M. Post-fire succession of collembolan communities in a northern hardwood forest. *Eur. J. Soil Biol.* **2012**, *48*, 59–65. [CrossRef]
11. Fernández-García, V.; Fulé, P.Z.; Marcos, E.; Calvo, L. The role of fire frequency and severity on the regeneration of Mediterranean serotinous pines under different environmental conditions. *For. Ecol. Manag.* **2019**, *444*, 59–68. [CrossRef]
12. Belcher, C.M. *Fire Phenomena and the Earth System: An Interdisciplinary Guide to Fire Science*; John Wiley & Sons: Hoboken, NJ, USA, 2013. [CrossRef]

13. Chowdhury, E.H.; Hassan, Q.K. Operational perspective of remote sensing-based forest fire danger forecasting systems. *ISPRS J. Photogramm. Remote Sens.* **2015**, *104*, 224–236. [CrossRef]

14. Ahmed, M.R.; Hassan, Q.K.; Abdollahi, M.; Gupta, A. Processing of near real time land surface temperature and its application in forecasting forest fire danger conditions. *Sensors* **2020**, *20*, 984. [CrossRef] [PubMed]

15. Ghaderpour, E.; Vujadinovic, T. The potential of the least-squares spectral and cross-wavelet analyses for near-real-time disturbance detection within unequally spaced satellite image time series. *Remote Sens.* **2020**, *12*, 2446. [CrossRef]

16. Abdollahi, M.; Hassan, Q.K.; Chowdhury, E.H.; Gupta, A. Exploring the relationships between topographical elements and forest fire occurrences in Alberta, Canada. In *Remote Sensing of Hydro-Meteorological Hazards*; Petropoulos, G., Islam, T., Eds.; CRC Press: Boca Raton, FL, USA, 2017; Chapter 13.

17. Ager, A.A.; Vaillant, N.M.; Finney, M.A. Integrating fire behavior models and geospatial analysis for wildland fire risk assessment and fuel management planning. *J. Combust.* **2011**, *2011*, 572452. [CrossRef]

18. Khakzad, N.; Dadashzadeh, M.; Reniers, G. Quantitative assessment of wildfire risk in oil facilities. *J. Environ. Manag.* **2018**, *223*, 433–443. [CrossRef] [PubMed]

19. Ma, W.; Feng, Z.; Cheng, Z.; Chen, S.; Wang, F. Identifying forest fire driving factors and related impacts in china using random forest algorithm. *Forests* **2020**, *11*, 507. [CrossRef]

20. Abdollahi, M.; Dewan, A.; Hassan, Q.K. Applicability of remote sensing-based vegetation water content in modeling lightning-caused forest fire occurrences. *ISPRS Int. J. Geoinf.* **2019**, *8*, 143. [CrossRef]

21. Nation, Food and Agriculture Organization of the United Nations. REDD+ Reducing Emissions from Deforestation and Forest Degradation. Available online: https://www.fao.org/redd/news/detail/en/c/1399089/ (accessed on 16 March 2022).

22. Calder, W.J.; Shuman, B. Extensive wildfires, climate change, and an abrupt state change in subalpine ribbon forests, Colorado. *Ecology* **2017**, *98*, 2585–2600. [CrossRef]

23. Stevens-Rumann, C.S.; Kemp, K.B.; Higuera, P.E.; Harvey, B.J.; Rother, M.T.; Donato, D.C.; Morgan, P.; Veblen, T.T. Evidence for declining forest resilience to wildfires under climate change. *Ecol. Lett.* **2018**, *21*, 243–252. [CrossRef] [PubMed]

24. Ardakani, A.; Valadanzooj, M.J.; Mansourian, A. Spatial analysis of fire potential in Iran different region by using RS and GIS. *J. Environ. Stud.* **2010**, *35*, 25–34.

25. Jaafari, A.; Pourghasemi, H.R. Factors influencing regional-scale wildfire probability in Iran: An application of random forest and support vector machine. In *Spatial Modeling in GIS and R for Earth and Environmental Sciences*; Elsevier: Amsterdam, The Netherlands, 2019; pp. 607–619.

26. Abdollahi, M.; Islam, T.; Gupta, A.; Hassan, Q.K. An advanced forest fire danger forecasting system: Integration of remote sensing and historical source of ignition data. *Remote Sens.* **2018**, *10*, 923. [CrossRef]

27. Adab, H.; Kanniah, K.D.; Solaimani, K. Modeling forest fire risk in the northeast of Iran using remote sensing and GIS techniques. *Nat. Hazards* **2013**, *65*, 1723–1743. [CrossRef]

28. Adab, H.; Kanniah, K.D.; Solaimani, K.; Sallehuddin, R. Modelling static fire hazard in a semi-arid region using frequency analysis. *Int. J. Wildland Fire* **2015**, *24*, 763–777. [CrossRef]

29. Tao, C.; Huang, S.S.; Brown, G. The impact of festival participation on ethnic identity: The case of Yi torch festival. *Event Manag.* **2020**, *24*, 527–536. [CrossRef]

30. Alkhatib, A.A. A review on forest fire detection techniques. *Int. J. Distrib. Sens. Netw.* **2014**, *10*, 1–12. [CrossRef]

31. Talebi, K.S.; Sajedi, T.; Pourhashemi, M. *Forests of Iran: A Treasure from the Past, a Hope for the Future*; Springer: Dordrecht, The Netherlands; Heidelberg, Gernamy; New York, NY, USA; London, UK, 2014; p. 152. [CrossRef]

32. Eskandari, S. Fire of Iranian forests, consequences, opposition methods and solutions. *Hum. Environ.* **2021**, *19*, 175–187.

33. Hedayati, N.; Joneidi, H.; Ebrahimi Mohammadi, S. Fire risk assessment of Kurdistan province natural areas using statistical index method. *J. Nat. Environ.* **2019**, *72*, 403–416.

34. Attarod, P.; Rostami, F.; Dolatshahi, A.; Sadeghi, S.; Amiri, G.Z.; Bayramzadeh, V. Do changes in meteorological parameters and evapotranspiration affect declining oak forests of Iran? *J. For. Sci.* **2016**, *62*, 553–561. [CrossRef]

35. Attarod, P.; Sadeghi, S.; Pypker, T.; Bayramzadeh, V. Oak trees decline; a sign of climate variability impacts in the west of Iran. *Casp. J. Environ. Sci.* **2017**, *15*, 373–384.

36. Moradi, B.; Ravanbakhsh, H.; Meshki, A.; Shabanian, N. The effect of fire on vegetation structure in Zagros forests (Case Study: Sarvabad, Kurdistan province). *Iran. J. For.* **2016**, 8, 381–392.

37. Preisler, H.K.; Ager, A. Forest-fire models. In *Encyclopedia of Environmetrics*; El-Shaarawi, A.H.; Piegorsch, W.W., Eds.; John Wiley & Sons: Hoboken, NJ, USA, 2013. [CrossRef]

38. Naderpour, M.; Rizeei, H.M.; Khakzad, N.; Pradhan, B. Forest fire induced Natech risk assessment: A survey of geospatial technologies. *Reliab. Eng. Syst. Saf.* **2019**, *191*, 106558. [CrossRef]

39. Ljubomir, G.; Pamučar, D.; Drobnjak, S.; Pourghasemi, H.R. Modeling the spatial variability of forest fire susceptibility using geographical information systems and the analytical hierarchy process. In *Spatial Modeling in GIS and R for Earth and Environmental Sciences*; Elsevier: Amsterdam, The Netherlands, 2019; pp. 337–369.

40. Sivrikaya, F.; Küçük, Ö. Modeling forest fire risk based on GIS-based analytical hierarchy process and statistical analysis in Mediterranean region. *Ecol. Inform.* **2022**, *68*, 101537. [CrossRef]

41. Moayedi, H.; Mehrabi, M.; Bui, D.T.; Pradhan, B.; Foong, L.K. Fuzzy-metaheuristic ensembles for spatial assessment of forest fire susceptibility. *J. Environ. Manag.* **2020**, *260*, 109867. [CrossRef] [PubMed]

42. Ramsay, J.O.; Silverman, B.W. *Functional Data Analysis*, 2nd ed.; Springer: New York, NY, USA, 2005.

43. Achu, A.; Thomas, J.; Aju, C.; Gopinath, G.; Kumar, S.; Reghunath, R. Machine-learning modelling of fire susceptibility in a forest-agriculture mosaic landscape of southern India. *Ecol. Inform.* **2021**, *64*, 101348. [CrossRef]

44. Singh, M.; Huang, Z. Analysis of forest fire dynamics, distribution and main drivers in the Atlantic Forest. *Sustainability* **2022**, *14*, 992. [CrossRef]

45. de Santana, R.O.; Delgado, R.C.; Schiavetti, A. Modeling susceptibility to forest fires in the Central Corridor of the Atlantic Forest using the frequency ratio method. *J. Environ. Manag.* **2021**, *296*, 113343. [CrossRef] [PubMed]

46. Hong, H.; Naghibi, S.A.; Moradi Dashtpagerdi, M.; Pourghasemi, H.R.; Chen, W. A comparative assessment between linear and quadratic discriminant analyses (LDA-QDA) with frequency ratio and weights-of-evidence models for forest fire susceptibility mapping in China. *Arab. J. Geosci.* **2017**, *10*, 167. [CrossRef]

47. Abedi Gheshlaghi, H.; Feizizadeh, B.; Blaschke, T. GIS-based forest fire risk mapping using the analytical network process and fuzzy logic. *J. Environ. Plan. Manag.* **2020**, *63*, 481–499. [CrossRef]

48. Sari, F. Forest fire susceptibility mapping via multi-criteria decision analysis techniques for Mugla, Turkey: A comparative analysis of VIKOR and TOPSIS. *For. Ecol. Manag.* **2021**, *480*, 118644. [CrossRef]

49. Amatulli, G.; Peréz-Cabello, F.; de la Riva, J. Mapping lightning/human-caused wildfires occurrence under ignition point location uncertainty. *Ecol. Model.* **2007**, *200*, 321–333. [CrossRef]

50. Tariq, A.; Shu, H.; Siddiqui, S.; Mousa, B.; Munir, I.; Nasri, A.; Waqas, H.; Lu, L.; Baqa, M.F. Forest fire monitoring using spatial-statistical and Geo-spatial analysis of factors determining forest fire in Margalla Hills, Islamabad, Pakistan. *Geomat. Nat. Hazards Risk* **2021**, *12*, 1212–1233. [CrossRef]

51. Ghaderpour, E.; Pagiatakis, S.D.; Hassan, Q.K. A survey on change detection and time series analysis with applications. *Appl. Sci.* **2021**, *11*, 6141. [CrossRef]

52. Lautenberger, C. Wildland fire modeling with an Eulerian level set method and automated calibration. *Fire Saf. J.* **2013**, *62*, 289–298. [CrossRef]

53. Dashti, S.; Amini, J.; Ahmadi Sani, N.; Javanmard, A. Zoning areas prone to fire occurrences in the forest ecosystems of North Zagros (Case study: Sardasht forests in West Azarbaijan). *J. Nat. Environ. Hazards* **2022**, *10*, 105–126.

54. Eskandari, S.; Pourghasemi, H.R.; Tiefenbacher, J.P. Relations of land cover, topography, and climate to fire occurrence in natural regions of Iran: Applying new data mining techniques for modeling and mapping fire danger. *For. Ecol. Manag.* **2020**, *473*, 118338. [CrossRef]

55. Jaafari, A.; Gholami, D.M.; Zenner, E.K. A Bayesian modeling of wildfire probability in the Zagros Mountains, Iran. *Ecol. Inform.* **2017**, *39*, 32–44. [CrossRef]

56. Regmi, N.R.; Giardino, J.R.; Vitek, J.D. Modeling susceptibility to landslides using the weight of evidence approach: Western Colorado, USA. *Geomorphology* **2010**, *115*, 172–187. [CrossRef]

57. Jahdi, R.; Salis, M.; Darvishsefat, A.A.; Alcasena, F.; Mostafavi, M.A.; Etemad, V.; Lozano, O.M.; Spano, D. Evaluating fire modelling systems in recent wildfires of the Golestan National Park, Iran. *Forestry* **2016**, *89*, 136–149. [CrossRef]

58. Eskandari, S.; Chuvieco, E. Fire danger assessment in Iran based on geospatial information. *Int. J. Appl. Earth Obs. Geoinf.* **2015**, *42*, 57–64. [CrossRef]

59. Forests, Range, and Watershed Management Organization. Area and vegetation Map. Area of Natural Resources Areas by Provinces. Available online: https://frw.ir/ (accessed on 16 March 2022).

60. Alvares, C.A.; Stape, J.L.; Sentelhas, P.C.; Gonçalves, J.d.M.; Sparovek, G. Köppen's climate classification map for Brazil. *Meteorol. Z.* **2013**, *22*, 711–728. [CrossRef]

61. NASA Earth Data—Alaska Satellite Facility (ASF). Available online: https://vertex.daac.asf.alaska.edu/ (accessed on 16 March 2022).

62. Whelan, R. *The Ecology of Fire*; Cambridge University Press: Cambridge, UK, 1995; p. 346.

63. Balzter, H.; Gerard, F.F.; George, C.T.; Rowland, C.S.; Jupp, T.E.; McCallum, I.; Shvidenko, A.; Nilsson, S.; Sukhinin, A.; Onuchin, A. Impact of the Arctic Oscillation pattern on interannual forest fire variability in Central Siberia. *Geophys. Res. Lett.* **2005**, *32*, L14709. [CrossRef]

64. Carrara, A.; Crosta, G.; Frattini, P. Geomorphological and historical data in assessing landslide hazard. *Earth Surf. Process. Landforms* **2003**, *28*, 1125–1142. [CrossRef]

65. Roodposhti, M.S.; Safarrad, T.; Shahabi, H. Drought sensitivity mapping using two one-class support vector machine algorithms. *Atmos. Res.* **2017**, *193*, 73–82. [CrossRef]

66. Zhang, K.; Wu, X.; Niu, R.; Yang, K.; Zhao, L. The assessment of landslide susceptibility mapping using random forest and decision tree methods in the Three Gorges Reservoir area, China. *Environ. Earth Sci.* **2017**, *76*, 1–20. [CrossRef]

67. Dube, F.; Nhapi, I.; Murwira, A.; Gumindoga, W.; Goldin, J.; Mashauri, D. Potential of weight of evidence modelling for gully erosion hazard assessment in Mbire District–Zimbabwe. *Phys. Chem. Earth. Parts A/B/C* **2014**, *67*, 145–152. [CrossRef]

68. Song, K.-Y.; Oh, H.-J.; Choi, J.; Park, I.; Lee, C.; Lee, S. Prediction of landslides using ASTER imagery and data mining models. *Adv. Space Res.* **2012**, *49*, 978–993. [CrossRef]

69. van Westen, C.J. *Statistical Landslide Hazard Analysis, ILWIS 2.1 for Windows Application Guide*; ITC Publication: Enschede, The Netherlands, 1997; pp. 73–84.

70. Liuzzo, L.; Sammartano, V.; Freni, G. Comparison between different distributed methods for flood susceptibility mapping. *Water Resour. Manag.* **2019**, *33*, 3155–3173. [CrossRef]
71. Pontius, R.G., Jr.; Schneider, L.C. Land-cover change model validation by an ROC method for the Ipswich watershed, Massachusetts, USA. *Agric. Ecosyst. Environ.* **2001**, *85*, 239–248. [CrossRef]
72. Mukaka, M.M. A guide to appropriate use of correlation coefficient in medical research. *Malawi Med. J.* **2012**, *24*, 69–71. [PubMed]
73. Hinkle, D.; Wiersma, W.; Jurs, S. *Applied Statistics for the Behavioral Sciences*; Houghton Mifflin, Boston, MA, USA, 2003; Volume 663.
74. Jin, X.-Y.; Jin, H.-J.; Iwahana, G.; Marchenko, S. S.; Luo, D.-L.; Li, X.-Y.; Liang, S.-H. Impacts of climate-induced permafrost degradation on vegetation: A review. *Adv. Clim. Chang. Res.* **2021**, *12*, 29–47. [CrossRef]
75. Schmidt, I.B.; Moura, L.C.; Ferreira, M.C.; Eloy, L.; Sampaio, A.B.; Dias, P.A.; Berlinck, C.N. Fire management in the Brazilian savanna: First steps and the way forward. *J. Appl. Ecol.* **2018**, *55*, 2094–2101. [CrossRef]
76. Kayet, N.; Chakrabarty, A.; Pathak, K.; Sahoo, S.; Dutta, T.; Hatai, B.K. Comparative analysis of multi-criteria probabilistic FR and AHP models for forest fire risk (FFR) mapping in Melghat Tiger Reserve (MTR) forest. *J. For. Res.* **2020**, *31*, 565–579. [CrossRef]
77. Hong, H.; Jaafari, A.; Zenner, E. K. Predicting spatial patterns of wildfire susceptibility in the Huichang County, China: An integrated model to analysis of landscape indicators. *Ecol. Indic.* **2019**, *101*, 878–891. [CrossRef]
78. Koutsias, N.; Xanthopoulos, G.; Founda, D.; Xystrakis, F.; Nioti, F.; Pleniou, M.; Mallinis, G.; Arianoutsou, M. On the relationships between forest fires and weather conditions in Greece from long-term national observations (1894–2010). *Int. J. Wildland Fire* **2012**, *22*, 493–507. [CrossRef]
79. Wu, Z.; He, H.S.; Yang, J.; Liang, Y. Defining fire environment zones in the boreal forests of northeastern China. *Sci. Total Environ.* **2015**, *518*, 106–116. [CrossRef] [PubMed]
80. Balch, J.K.; Brando, P.M.; Nepstad, D.C.; Coe, M.T.; Silvério, D.; Massad, T.J.; Davidson, E.A.; Lefebvre, P.; Oliveira-Santos, C.; Rocha, W. The susceptibility of southeastern Amazon forests to fire: Insights from a large-scale burn experiment. *Bioscience* **2015**, *65*, 893–905. [CrossRef]
81. Cawson, J.G.; Duff, T.J.; Tolhurst, K.G.; Baillie, C.C.; Penman, T.D. Fuel moisture in Mountain Ash forests with contrasting fire histories. *For. Ecol. Manag.* **2017**, *400*, 568–577. [CrossRef]
82. Juliev, M.; Mergili, M.; Mondal, I.; Nurtaev, B.; Pulatov, A.; Hübl, J. Comparative analysis of statistical methods for landslide susceptibility mapping in the Bostanlik District, Uzbekistan. *Sci. Total Environ.* **2019**, *653*, 801–814. [CrossRef] [PubMed]
83. Eugenio, F.C.; dos Santos, A.R.; Fiedler, N.C.; Ribeiro, G.A.; da Silva, A.G.; dos Santos, Á.B.; Paneto, G.G.; Schettino, V. R. Applying GIS to develop a model for forest fire risk: A case study in Espírito Santo, Brazil. *J. Environ. Manag.* **2016**, *173*, 65–71. [CrossRef] [PubMed]
84. Catry, F.; Rego, F.; Moreira, F.; Fernandes, P.; Pausas, J. Post-fire tree mortality in mixed forests of central Portugal. *For. Ecol. Manag.* **2010**, *260*, 1184–1192. [CrossRef]
85. Martínez-Fernández, J.; Chuvieco, E.; Koutsias, N. Modelling long-term fire occurrence factors in Spain by accounting for local variations with geographically weighted regression. *Nat. Hazards Earth Syst. Sci.* **2013**, *13*, 311–327. [CrossRef]